Supplementary Information

Chiral zero-dimensional hybrid organic–inorganic metal halides based on nipecotic acids and tetrabromocuprate

Xianran Wang,‡[a,b] Yuying Wu,‡[c] Feng Gao[*a] and Youfu Wang[*b]

[a.] State Key Laboratory of Featured Metal Materials and Life-cycle Safety for Compo-site Structures, School of Resources, Environment and Materials, Guangxi University, Nanning 530004, P. R. China.
E-mail: gaofeng@gxu.edu.cn

[b.] School of Chemistry and Chemical Engineering, Frontiers Science Center for Transformative Molecules, Shanghai Jiao Tong University, Shanghai 200240, P. R. China.
E-mail: wyfown@sjtu.edu.cn

[c.] School of Electrical Engineering, Shanghai DianJi University, Shanghai 201306, P. R. China.

‡ XR.W and YY. W. contributed equally to this work.

Materials Synthesis and Characterizations

Materials Synthesis and Characterizations

Materials

(S)-(+)-NA, (R)-(-)-NA, copper bromide ($CuBr_2$) and hydrobromic acid in analytically pure were purchased from Adamas Reagent Company and used directly without purification.

Synthesis of chiral hybrid organic–inorganic metal halides

[*S*-NA]$_2$[$CuBr_4$] and [*R*-NA]$_2$[$CuBr_4$] single crystals were synthesized at room temperature using the commonly used solution evaporation method. The specific method was as follows: NA (5 mmol) and $CuBr_2$ (2.5 mmol) were first dissolved in an appropriate amount of water and hydrobromic acid (5 mL), respectively, and then the aqueous solution and the acid solution are fully mixed to obtain the purple black mixed solution. The mixed solution was placed in a fume hood and evaporated slowly at common atmosphere. After a few days, small black crystals were observed, indicating that the target single crystals were obtained.

Structural Characterization

Single Crystal X-ray Diffraction (SCXRD) data has been acquired on a D8 VENTURE type of diffractometer with an X-ray source: a high intensity microfocused rotating anode source, Cu Kα target. The appropriate single crystals were scrutinized with an optical microscope and affixed to the fine glass fibers. Fourier synthesis calculations were derived by parsing and completing the single-crystal structure information using an adapted version of the SHELXL-97 program included in the OLEX2 package.

Powder X-ray diffraction (PXRD) data were collected at a D8 Advance-type X-ray diffractometer, Cu Kα palladium, scan range 2θ is 5~90°. The XPS of individual crystals were recorded on the Nexsa instrument equipped with a monochromatic Al Kα microfocus X-ray source. An instrument model FEIApreo 2S HiVac field emission scanning electron microscope, with an X-ray energy spectrometer, was used to observe the microstructure and energy spectrum acquisition.

The Raman spectra for the single crystals were acquired with the DXR Raman spectrometer. The Raman spectra were recorded from polycrystalline samples in the 3500~50 cm^{-1} range using a physical argon ion laser with a 523 nm spectral line. The solid-state CD spectroscopy measurements were performed on a Jasco-1500 CD polarization spectrometer. At 19.85 °C, the measurement wavelength range was 200~300 nm. The synthesized crystals were first

dissolved in DMF solution, and then coated on the quartz substrate to prepare a continuous [*S*-NA]$_2$[CuBr$_4$] and [*R*-NA]$_2$[CuBr$_4$] film for CD spectroscopy.

Spectroscopic measurement

The ultraviolet-visible spectra (UV-vis) of the single crystals [*S*-NA]$_2$[CuBr$_4$] and [*R*-NA]$_2$[CuBr$_4$] were measured within the range of 200-800 nm with a conventional UV-visible absorption spectrometer Lambda 750S in a room temperature, and spectrally pure $BaSO_4$ solid powders were firstly tested, which was used for calibration. After the test, a small amount of the sample was flattened in the center of a mold with $BaSO_4$ solid powder and tested.

The Raman spectra for the single crystals were acquired with the DXR Raman spectrometer. The Raman spectra were recorded from polycrystalline samples in the 3500~50 cm^{-1} range using a physical argon ion laser with a 523 nm spectral line. The solid-state CD spectroscopy measurements were performed on a Jasco-1500 CD polarization spectrometer. At 19.85 °C, the measurement wavelength range was 200~300 nm. The synthesized crystals were first dissolved in DMF solution, and then coated on the quartz substrate to prepare a continuous [*S*-NA]$_2$[CuBr$_4$] and [*R*-NA]$_2$[CuBr$_4$] film for CD spectroscopy.

Thermal test

The differential scanning calorimetry (DSC) measurements were made on the NETZSCH DSC 214 instrument. The thermal properties of single crystal [*S*-NA]$_2$[CuBr$_4$] and [*R*-NA]$_2$[CuBr$_4$] were studied by DSC. The temperature range was -70~150 °C and the DSC changes of the samples during cooling and heating were recorded at a temperature variation occurs at a speed of 10 °C/min.

Thermogravimetric analysis (TGA) and DTG measurements were performed on the NETZSCH TG 209F1 Libra instrument by placing approximately 10 mg of powder in an alumina crucible with a temperature scale of 30~910 °C. The sample was heated at the speed of 10 °C/min under nitrogen.

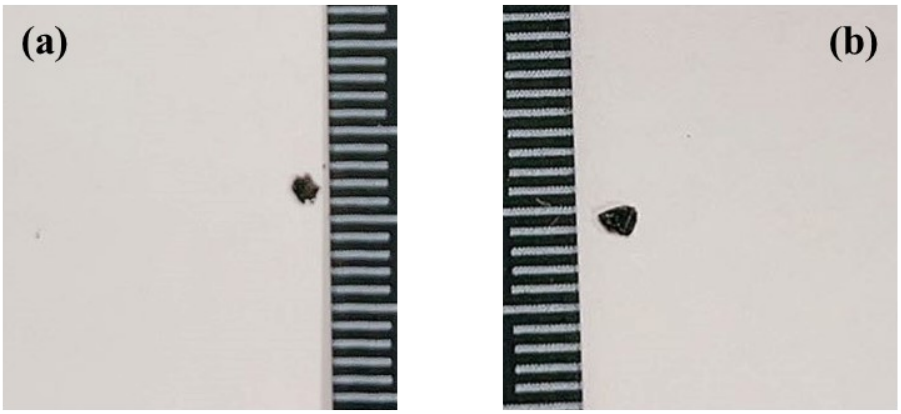

Figure S1. Photograph of (a) [*S*-NA]$_2$[CuBr$_4$] and (b) [*R*-NA]$_2$[CuBr$_4$].

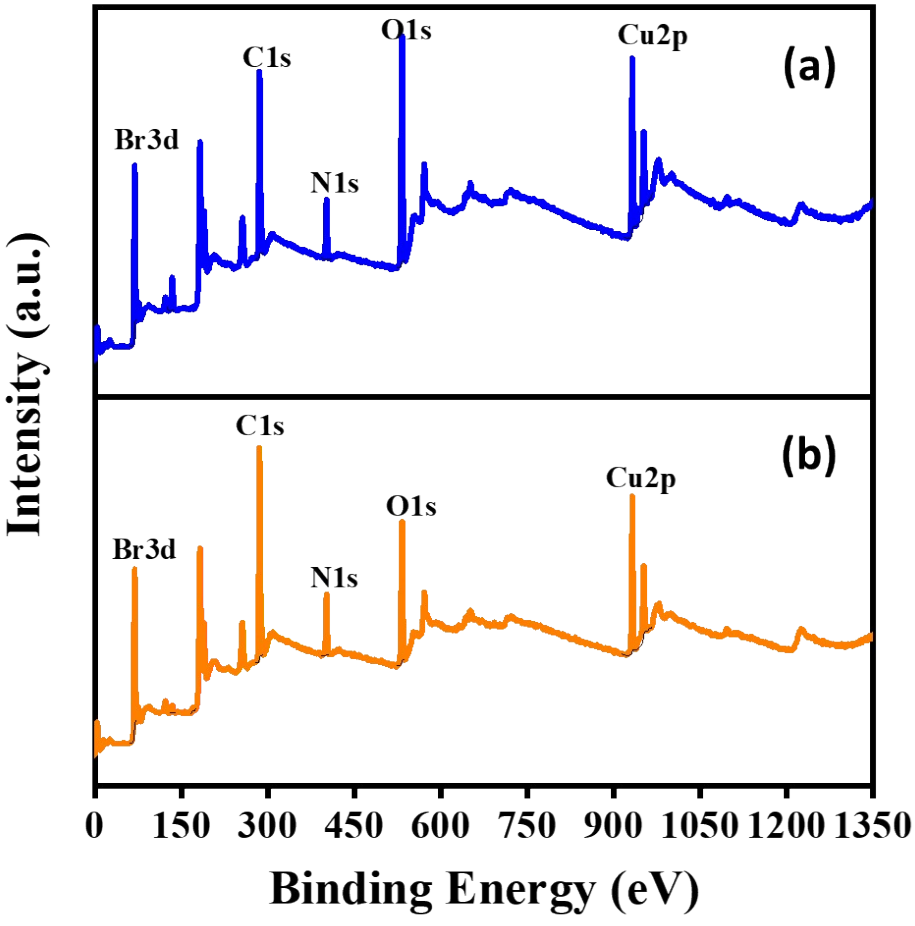

Figure S2. XPS spectra of (a) [*S*-NA]$_2$[CuBr$_4$] and (b) [*R*-NA]$_2$[CuBr$_4$].

(a)

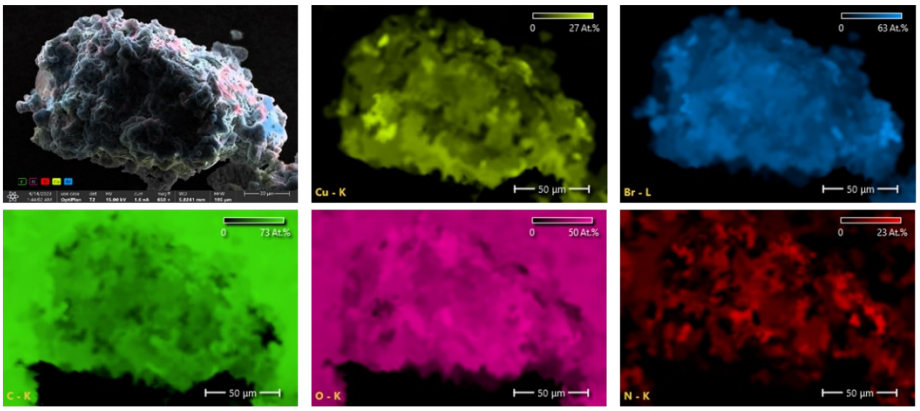

Element	Atomic %
N	2.8
Br	7.9
C	65.0
O	21.4
Cu	2.9

(b)

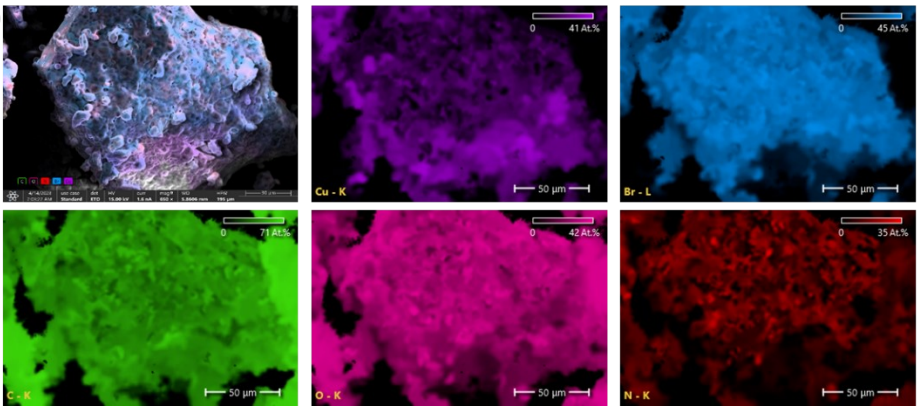

Element	Atomic %
N	5.6
Br	3.8
C	71.4
O	18.1
Cu	1.2

Figure S3. SEM and EDS mapping images of (a) [*S*-NA]$_2$[CuBr$_4$] and (b) [*R*-NA]$_2$[CuBr$_4$].

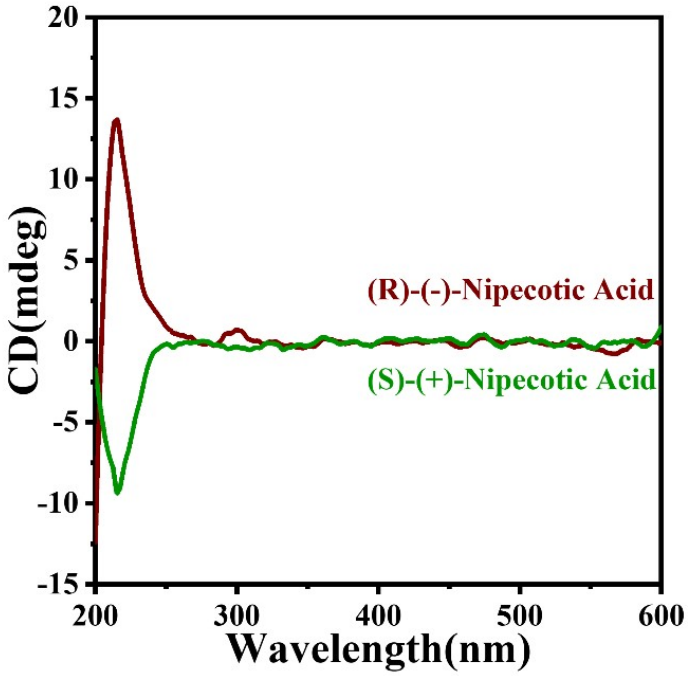

Figure S4. CD spectra of (S)-(+)-NA and (R)-(-)-NA.

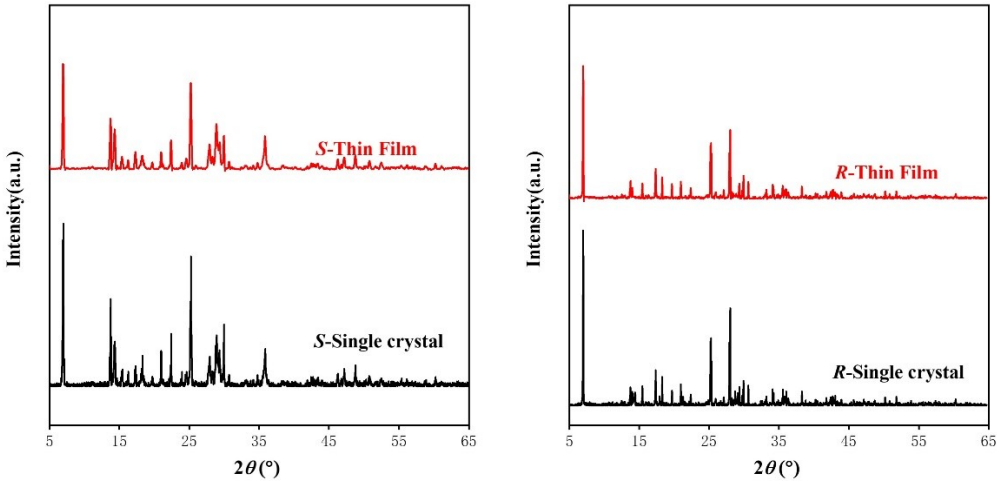

Figure S5. Powder XRD patterns of as-prepared (S)-(+)-NA and (R)-(-)-NA thin films overlapped with that of the (S)-(+)-NA and (R)-(-)-NA single crystals.

Table S1. Crystal data and structure refinement for [*S*-NA]$_2$[CuBr$_4$] and [*R*-NA]$_2$[CuBr$_4$].

Empirical formula	[*S*-$C_6H_{12}NO_2$]$_2$[$CuBr_4$]	[*R*-$C_6H_{12}NO_2$]$_2$[$CuBr_4$]
Formula weight/g mol^{-1}	643.51	643.51
Crystal system	orthorhombic	orthorhombic
Space group	$C222_1$	$C222_1$
T/K	296	296
a/ Å	8.3889(5)	9.8431(10)
b/ Å	9.8846(7)	8.4200(9)
c/ Å	25.0684(17)	25.190(2)
α/β/γ(°)	90/90/90	90/90/90
Volume/ Å^3	2078.7(2)	2087.7(3)
Z	4	4
Density/g cm^{-3}	2.056	2.047
Radiation	CuKα (λ = 1.54178)	CuKα (λ = 1.54184)
μ/mm^{-1}	10.646	10.600
F(000)	1244.0	1244.0
Thetarange(data collection)	13.846 to 136.652	7.018 to 136.68
Index ranges	$-10 \le h \le 10$, $-11 \le k \le 11$, $-29 \le l \le 30$	$-11 \le h \le 11$, $-9 \le k \le 10$, $-30 \le l \le 30$
Reflections colleted	15127	10882
Independent reflections	1902 [R_{int} =0.0501, R_{sigma} =0.0282]	1909 [R_{int} =0.0466, R_{sigma}= 0.0358]
Data/restrants/parameters	1902/50/163	1909/56/160
Goodness-of-fit on F^2	1.054	1.097
Final R indexes[I>=2σ(I)]	R_1 = 0.0294, wR_2 = 0.0789	R_1 =0.0370, wR_2 =0.1023
Final R indexes[all data]	R_1 = 0.0325, wR_2 = 0.0806	R_1 = 0.0383, wR_2 = 0.1039
Largest diff.peak/hole/e Å^{-3}	0.33/-0.33	0.39/-0.59
Flack parameter	0.08(5)	0.22(7)

Table S2. Bond lengths for [*S*-NA]$_2$[CuBr$_4$].

Atom	Atom	Length/Å	Atom	Atom	Length/Å
Br_5	Cu_1^1	2.393(2)	C_2	C_3	1.505(9)
Br_5	Cu_1	2.393(2)	C_2	C_1	1.514(7)
Br_5	Cu_2	2.2902(7)	O_2	C_1	1.252(7)
Br_5	Cu_2^1	2.2902(7)	N_4	C_3	1.490(7)
Br_5	Cu_3	2.417(6)	N_4	C_4	1.465(8)
Br_5	Cu_3^1	2.491(6)	C_6	C_5	1.518(9)
Br_5	Cu_4	2.447(13)	C_4	C_5	1.492(10)
Br_1	Cu_1^1	2.395(4)	Cu_2	Cu_2^1	0.00(2)
Br_1	Cu_1	2.395(4)	Cu_2	Br_2	2.469(10)
Br_5	Cu_1^1	2.393(2)	C_2	C_3	1.505(9)
Br_5	Cu_1	2.393(2)	C_2	C_1	1.514(7)
C_2	C_6	1.509(8)	Cu_3	Br_3	1.93(5)

[1]1-X,+Y,1/2-Z; [2]-1/2+X,-1/2+Y,+Z

Table S3. Bond lengths for [*R*-NA]$_2$[CuBr$_4$].

Atom	Atom	Length/Å	Atom	Atom	Length/Å
Br_5	Cu_2	2.2984(11)	C_2	C_1	1.510(11)
Br_5	Cu_3	2.386(5)	C_2	C_3	1.493(11)
Br_5	Cu_3^1	2.538(5)	C_5	C_4	1.500(12)
Br_5	Cu_1	2.433(5)	C_5	N_1	1.464(10)
Br_5	Cu_4	2.347(17)	C_1	N_1	1.504(9)
Cu_2	Br_2^1	2.444(12)	C_3	C_4	1.538(10)
Cu_2	Br_2	2.444(12)	Br_4	Cu_4	2.48(4)
O_1	C_6	1.265(9)	Cu_3	Br_3	1.96(4)
O_2	C_6	1.244(8)	Br_1	Cu_1	2.323(10)
C_2	C_6	1.504(8)			

[1]+X,1-Y,1-Z

Table S4. Bond angles for [*S*-NA]$_2$[CuBr$_4$].

Atom	Atom	Atom	Angle/°	Atom	Atom	Atom	Angle/°
Cu_1	Br_5	Cu_1^1	0.0(4)	N_4	C_4	C_5	111.5(6)
Cu_1^1	Br_5	Cu_3^1	27.78(19)	C_4	C_5	C_6	112.3(5)
Cu_1	Br_5	Cu_3^1	27.78(19)	Br_5	Cu_2	Br_5^1	179.3(6)
Cu_2^1	Br_5	Cu_2	0.0(6)	Br_5	Cu_2	Br_2	88.7(2)
Cu_1^1	Br_1	Cu_1	0.000(1)	Br_5^1	Cu_2	Br_2	91.7(2)
Br_5	Cu_1	Br_5^1	146.3(4)	Br_5^1	Cu_2	Br_2^1	88.7(2)
Br_5^1	Cu_1	Br_1^1	96.75(4)	Br_5	Cu_2	Br_2^1	91.7(2)
Br_5^1	Cu_1	Br_1	97.88(5)	Cu_2^1	Cu_2	Br_5	0(10)
Br_5	Cu_1	Br_1	96.75(4)	Cu_2^1	Cu_2	Br_2^1	0(10)
Br_5	Cu_1	Br_1^1	97.88(5)	Cu_2^1	Cu_2	Br_2	0(10)
Br_1^1	Cu_1	Br_1	127.8(4)	Br_2	Cu_2	Br_2^1	108.4(6)
Cu_1^1	Cu_1	Br_5^1	0(10)	O_1	C_1	C_2	118.4(5)
Cu_1^1	Cu_1	Br_5	0(10)	O_1	C_1	O_2	124.6(5)
Cu_1^1	Cu_1	Br_1^1	0(10)	O_2	C_1	C_2	117.0(5)
Cu_1^1	Cu_1	Br_1	0(10)	Cu_2^1	Br_2	Cu_2	0.0(4)
C_6	C_2	C_1	109.3(4)	Br_5	Cu_3	Br_5^1	137.9(4)
C_3	C_2	C_6	110.9(5)	Br_3	Cu_3	Br_5	115.6(13)
C_3	C_2	C_1	111.3(5)	Br_5	Cu_4	Br_5^1	138.7(16)
C_4	N_4	C_3	113.5(5)	Br_4^1	Cu_4	Br_5	105.5(3)
C_2	C_6	C_5	110.3(5)	Br_4	Cu_4	Br_5	97.7(2)
N_4	C_3	C_2	109.4(5)	Br_4^1	Cu_4	Br_4	110.6(15)

[1]1-X,+Y,1/2-Z; [2]1/2+X,1/2+Y,+Z

Table S5. Bond angles for [*R*-NA]$_2$[CuBr$_4$].

Atom	Atom	Atom	Angle/°	Atom	Atom	Atom	Angle/°
Cu_1	Br_5	Cu_3^1	25.8(3)	C_5	C_4	C_3	111.4(6)
Br_5^1	Cu_2	Br_5	174.4(6)	Br_5	Cu_3	Br_5^1	137.6(3)
Br_5^1	Cu_2	Br_2^1	93.9(2)	Br_3	Cu_3	Br_5	119.7(10)
Br_5^1	Cu_2	Br_2	89.1(2)	Br_5^1	Cu_1	Br_5	141.3(7)
Br_5	Cu_2	Br_2^1	89.1(2)	Br_1	Cu_1	Br_5^1	96.61(13)
Br_5	Cu_2	Br_2	93.9(2)	Br_1^1	Cu_1	Br_5	96.61(13)
Br_2^1	Cu_2	Br_2	113.3(6)	Br_1	Cu_1	Br_5	104.69(19)
C_6	C_2	C_1	111.3(6)	Br_1^1	Cu_1	Br_5^1	104.69(19)
C_3	C_2	C_6	109.3(6)	Br_1^1	Cu_1	Br_1	112.3(8)
C_3	C_2	C_1	110.9(6)	Br_5^1	Cu_4	Br_5	156(4)
O_1	C_6	C_2	118.1(6)	Br_5^1	Cu_4	Br_4^1	94.9(6)
O_2	C_6	O_1	123.4(6)	Br_5	Cu_4	Br_4	94.9(6)
O_2	C_6	C_2	118.4(6)	Br_5	Cu_4	Br_4^1	96.5(6)
N_1	C_5	C_4	112.7(7)	Br_5^1	Cu_4	Br_4	96.5(6)
N_1	C_1	C_2	109.0(7)	Br_4^1	Cu_4	Br_4	123(3)
C_2	C_3	C_4	111.0(6)	C_5	N_1	C_1	113.0(6)

[1]+X,1-Y,1-Z